

Silica-Lipid Hybrid (SLH) Versus Non-lipid Formulations for Optimising the Dose-Dependent Oral Absorption of Celecoxib

Angel Tan · Andrew K. Davey · Clive A. Prestidge

Received: 20 January 2011 / Accepted: 23 February 2011 / Published online: 11 May 2011
© Springer Science+Business Media, LLC 2011

ABSTRACT

Purpose To investigate the dose linearity of celecoxib (CEL) pharmacokinetics from various non-lipid and lipid-based formulations; to probe the mechanisms of CEL absorption from a nano-structured silica-lipid hybrid (SLH) microparticle dosage form.

Methods Single-dose pharmacokinetic parameters of CEL were determined in fasted rats at dose levels of 5, 20 and 50 mg/kg in aqueous suspensions of pure CEL, Celebrex[®] and CEL-SLH microparticles formulated using medium-chain lipids (Miglyol 812 or Capmul MCM) and Aerosil[®] silica nanoparticles. An *in vitro* lipolysis model was used to characterise the dynamic solubilisation state of CEL under digesting conditions.

Results CEL-SLH formulations and Celebrex[®] consistently produced a 2-fold higher maximum plasma concentration (C_{max}) and bioavailability ($AUC_{0 \rightarrow \infty}$) than pure CEL in a dose-linear manner within the dose range of 5–50 mg/kg CEL ($R^2 > 0.8$). Lipolysis drug phase partition data indicate a 2.5–7.5-fold higher CEL solubilising capacity resulting from the digestion of SLH microparticles as compared to the simulated fasted state endogenous micelles. Strong correlations were obtained

between maximum CEL solubilisation levels during lipolysis and *in vivo* pharmacokinetic parameters ($R^2 > 0.9$).

Conclusions Collectively, the results highlight the potential of the SLH microparticles in enhancing the bioavailability of CEL in a dose-linear manner as facilitated by supersaturated solubilisation of CEL in the intestinal milieu.

KEY WORDS celecoxib · dose-dependent absorption
in vitro-in vivo correlations · lipid-based formulation · lipolysis

INTRODUCTION

Celecoxib (Celebrex[®], Pfizer/Pharmacia), chemically designated as 4-[5-(4-methylphenyl)-3-trifluoromethyl]-1-H-pyrazol-1-yl] benzenesulfonamide, is used primarily for the management of rheumatism, osteoarthritis and dysmenorrhea, as well as an adjuvant for treating familial adenomatous polyposis (1). Celecoxib (CEL) selectively inhibits the COX-2 enzyme and thus is regarded to be relatively safer than traditional non-steroidal anti-inflammatory drugs (NSAIDs) because of its minimal gastrointestinal side effects. Despite safety concerns with some COX-2 inhibitors, such as rofecoxib (Vioxx[®], Merck) and valdecoxib (Bextra[®], Pfizer), which were withdrawn by the drug companies due to increased risk of myocardial infarction (2), and the cancellation of registration of lumiracoxib (Prexige[®], Novartis) by the Australian Therapeutic Goods Administration due to serious liver side effects (3), CEL does not appear to have the toxicities associated with other drugs in its class.

Although CEL is generally well tolerated, it is poorly absorbed when administered orally in its original form. The bioavailability of CEL ranged between 64–88% when administered as aqueous solutions and 20–40% in its solid

A. Tan · C. A. Prestidge (✉)
Ian Wark Research Institute, ARC Special Research Centre for Particle and Material, Interfaces, University of South Australia
Mawson Lakes, SA 5095, Australia
e-mail: clive.prestidge@unisa.edu.au

A. Tan · A. K. Davey
Sansom Institute, School of Pharmacy and Medical Science
University of South Australia
Adelaide, SA 5000, Australia

A. K. Davey
School of Pharmacy, Griffith University
Gold Coast, QLD 4215, Australia

form in dogs (4). CEL, a weak acid ($pK_a \approx 11$), is classified as a Biopharmaceutics Classification Scheme (BCS) Class II drug (i.e. poor water solubility and high lipophilicity) with an aqueous solubility of 3–7 $\mu\text{g}/\text{ml}$ (at pH 7.0, 40°C) and an intermediate lipophilicity ($\log P \approx 3.5$) (5). As such, CEL exhibits a lack of linearity in its dose-pharmacokinetic profiles, particularly at doses above 200 mg in humans under fasting conditions, mainly due to erratic absorption via the oral route (1,6,7). While the bioavailability of CEL has been shown to increase up to five-fold in dogs in the fed state, high fat meals did not appear to increase CEL absorption to a clinically significant degree in humans, where co-administration of 200 mg CEL capsules (filled with water-soluble diluents) with a meal containing 75 g fat resulted in only a 10–20% increase in its absorption (4).

Lipid-based formulations are developed to mimic the post-prandial effect on the basis that lipid-based carriers potentially present the drugs in a molecularly dispersed or dissolved state during gastrointestinal transit, as well as inducing a series of physiological responses (e.g. increased biliary secretions) and biochemical changes (e.g. increased intestinal permeability) which favour drug absorption (8). Specific investigations that illuminate the precise role of various formulation lipids (e.g. tri/ di/ monoglycerides with different acyl chain length) in enhancing the oral absorption of CEL at various dose strengths have yet to be reported. There are several challenges that potentially compromise the therapeutic use of many lipid-based formulations, including the need to employ synthetic surfactants to facilitate dispersibility of some oily vehicles, the use of organic solvents in the manufacturing process, as well as the lack of solid dosage forms that normally gain better patient compliance and have a reasonably long shelf-life (9). Notwithstanding these problems, the availability of the 3–4% oral lipid-based products in the pharmaceutical market worldwide has supported the use of lipid-based technology in addressing the low bioavailability issue of BCS Class II drugs (10).

Lipid hybrid systems stabilised by silica nanoparticles have previously been shown to offer attractive physicochemical and biopharmaceutical advantages, including prolonged storage stability of lipid-based systems (11), protection of photosensitive drugs (12,13), as well as improved oral and dermal drug delivery (14–17). This paper describes for the first time the use of a nano-structured, porous silica-lipid hybrid (SLH) carrier as a novel solid-state lipid-based formulation to enhance the oral bioavailability of CEL in a dose-linear manner. This formulation originates from a simple oil-in-water emulsion (consisting of a dispersed oil phase in the presence of an emulsifier) which is subsequently encapsulated by a solid carrier prior to transformation into the dry microparticle form (14,15). Silica-based materials are effective in enhancing the dissolution and absorption of BCS

Class II drugs, mainly via preservation of the drug amorphous or molecularly dispersed form, as well as increased drug wettability in the aqueous medium (18–21). Importantly, the maintenance of a supersaturated state in the GI fluids also presents a driving force for enhanced drug absorption (22,23). This study extends our previous investigations on the CEL-SLH formulations and provides a detailed assessment on the dose-dependent absorption of CEL when delivered orally from various non-lipid and lipid-based formulations in a fasted rat model. The major aim was to determine if the SLH microparticle system produces a linear dose-pharmacokinetic response which renders a more predictable absorption for CEL in comparison with its original form. To examine the significance of post-lipolysis solubilisation on the absorption of CEL, a systematic *in vitro-in vivo* correlation was undertaken based on CEL phase partition under lipase-mediated digesting conditions. This provides an improved understanding of the mechanisms of drug release, solubilisation, and absorption from the SLH formulations.

MATERIALS AND METHODS

Materials

Celecoxib powder ($\geq 99.0\%$ purity) and Celebrex[®] capsules (100 mg celecoxib) were purchased from Chem-Pacific (USA) and Australian Pharmaceutical Industries (Australia), respectively. Miglyol 812, a mixture of saturated caprylic/capric (C_8/C_{12}) triglycerides, was supplied by Hamilton Laboratories (Australia). Capmul MCM, a C_8/C_{12} mono-diglyceride blend, was a generous gift obtained from Abitech Corporation (USA). Soybean lecithin ($>94\%$ phosphatidylcholine and $<2\%$ triglycerides) was purchased from BDH Merck (Australia). Hydrophilic fumed silica (Aerosil[®] 380) with a primary average diameter of 7 nm and a specific surface area of $380 \pm 30 \text{ m}^2/\text{g}$ was purchased from Evonik Degussa (Germany). Sodium taurodeoxycholate (NaTDC) 99%, Trizma maleate, type X-E L- α -lecithin (60% pure phosphatidylcholine, from dried egg yolk), porcine pancreatin extract (activity equivalent to $8 \times$ USP specification), 4-bromophenylboronic acid (4-BPB), calcium chloride dehydrate and sodium hydroxide pellets were purchased from Sigma-Aldrich (Australia). All other chemicals were of analytical grade and used as received. High purity (Milli-Q) water was used throughout the study.

Preparation of CEL-SLH Microparticles

Different types of CEL-SLH microparticles, designated as SLH-M (containing Miglyol 812) and SLH-C (containing

Capmul MCM), were fabricated as previously described (Fig. 1) (14). The equilibrium solubility of CEL in Capmul MCM and Miglyol 812 was pre-determined to be 1.1 ± 0.0 and $9.3 \pm 0.1\%$ (w/w), respectively, using the conventional shake-flask or batch agitation method (24). First, submicron oil-in-water emulsions (containing CEL in excess of its equilibrium solubility in lipids) were prepared by high pressure homogenisation (Avestin[®] EmulsiFlex-C5 Homogeniser, Canada) under a pressure of 1000 bar for 5–6 cycles. An aqueous dispersion of 5% (w/v) silica was added to the homogenised emulsions and tumbled for 12 h. The silica-stabilised emulsions were spray-dried (BÜCHI Mini Spray Dryer B-290, Switzerland) to produce powdery CEL-SLH microparticles under the following conditions: emulsion flow rate 5 ml/min, aspirator setting 10, air flow rate $0.6 \text{ m}^3/\text{min}$, inlet and outlet temperature 160°C and 65°C .

Physicochemical Characterisation of CEL-SLH Microparticles

The solid-state morphology of the CEL-SLH microparticles was examined by high resolution analytical scanning electron microscopy, SEM (CamScan CS44FE). Each sample was mounted on double-faced adhesive tape and sputter-coated with gold/palladium (60%:40%) prior to imaging at an accelerating voltage of 10 kV, spot size $10 \mu\text{m}$, and an aperture of $50 \mu\text{m}$.

The particle sizes of the CEL-SLH microparticles were characterised using laser diffraction (Malvern Mastersizer 2000, UK). Water (refractive index=1.33) was used as the dispersant, and the particle refractive index was pre-set as 1.45 for medium-chain lipids and silica particles. The zeta potentials of the CEL-SLH microparticles (5 mg/ml redispersed in phosphate buffer

0.05 M, pH 7.2) were characterised using phase analysis light scattering (PALS) (Malvern Zetasizer Nano ZS, UK). The samples were diluted 100-fold with water prior to measurement at 25°C .

The lipid content of the CEL-SLH microparticles was determined by thermogravimetric analysis (Hi-Res Modulated TGA 2950, TA Instruments Australia). Each microparticle sample (approximately 10 mg) was heated at a scanning rate of $10^\circ\text{C}/\text{min}$ from 20°C to 600°C under a nitrogen gas purge. The lipid content (both oils and lecithin) was evaporated in the range of $240\text{--}350^\circ\text{C}$, and the silica component remained thermally stable. After correction for the water content of spray-dried silica (previously determined to be $1.5 \pm 0.0\%$), the subtracted weight loss was computed by using the associated TA Universal Analysis software, and this corresponds to the lipid content of the microparticles.

The amount of CEL loaded into the SLH microparticles was determined by a solvent extraction method. The encapsulated CEL was extracted by dissolving 10 mg of the formulation powder in 4 ml methanol (which has been tested to give a $100 \pm 1\%$ extraction efficiency). The supernatant (0.5 ml) was taken, and the solvent was completely evaporated under a dry nitrogen stream at 30°C (Pierce Reacti-Therm[™] Heating Module, US). The resulting residue was re-dissolved in 10 ml of the HPLC mobile phase solution by vortex-mixing for 1 min, and centrifuged at $9400g$ for 15 min prior to HPLC analysis for CEL content. The degree of crystallinity of CEL was monitored by X-ray diffraction (XRD, Philips PW 1050/25, Netherlands). The CEL formulation samples were scanned between 10 and 50° (2θ) at 0.02° intervals at a rate of $0.05^\circ/\text{min}$. Co-K- α radiation (60 kV, 30 mA, 1.7902 \AA) were used with a $1/12^\circ$ collimation slit. Peak analysis was performed using the SIROQUANT V3 software.

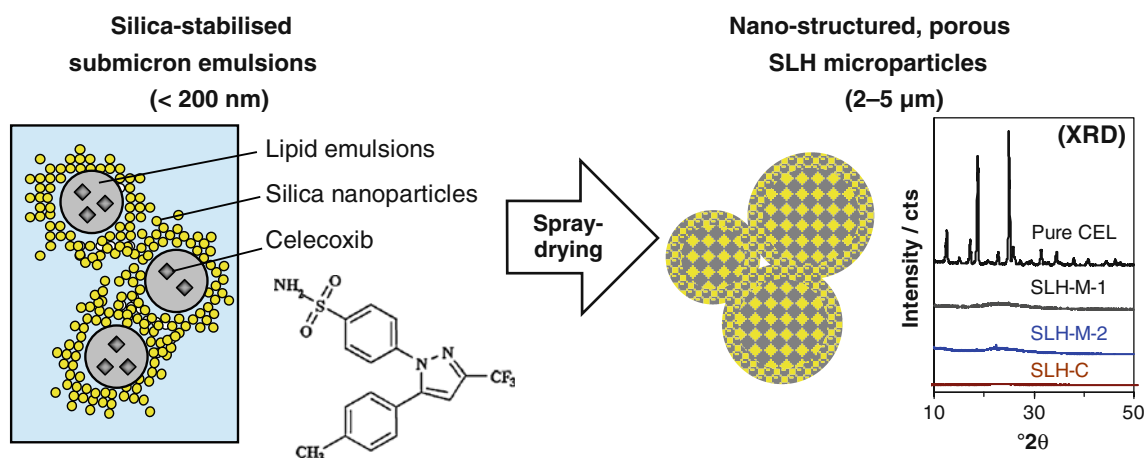


Fig. 1 Schematic representation of the formation of nano-structured, porous SLH microparticles from precursor submicron emulsions encapsulated by silica nanoparticles (drawing not according to scale).

In Vitro Lipolysis Study

Preparation of Lipid Digestion Medium

The fasted-state mixed micellar solution was prepared in the following sequence for producing a bile salt:phospholipids concentration of 5 mM:1.25 mM in the reaction mixture after enzyme additions: egg lecithin was first dissolved in chloroform (20 mg/ml), and the chloroform was evaporated under vacuum (BÜCHI Rotavapor-RE, Switzerland) to form a thin film of lecithin on the walls of a round-bottom flask; bile salt (i.e. NaTDC) and digestion buffer (consisting of 50 mM Trizma maleate (pH 7.5), 150 mM NaCl, and 5 mM CaCl₂·2H₂O) were added, and the mixture was stirred for ~12 h to produce a transparent (light yellow) micellar solution. The mixed micellar solutions were kept refrigerated (2–8°C) and used within 2 weeks of the day of preparation. Pancreatin extracts (containing pancreatic lipase, colipase and other non-specific lipolytic enzymes such as phospholipase A₂) were freshly prepared each day by stirring 1 g of porcine pancreatin powder in 5 ml of digestion buffer for 15 min, followed by centrifugation at 1600g (5°C) for 15 min. The supernatant phase was collected and stored on ice until use.

Digestion Experimental Procedure

The progress of lipid digestion was monitored for 60 min by using a TitraLab[®] 854 pH-stat titration apparatus (Radiometer Analytical, France) according to a previously established lipolysis model (25). A known quantity of lipid formulation (at a dose of 100 mg oil per 10 ml lipolysis volume) was initially dispersed in the buffered micellar solution (37°C), and the pH was re-adjusted to 7.50±0.01 with 0.1 M NaOH or HCl solution. Lipolysis was initiated by adding 1 ml of pancreatin extract per 10 ml of lipolysis volume to produce a final lipase concentration of ~1000 TBU per ml of lipolysis volume. Free fatty acids (FFA) produced in the reaction vessel were titrated with 0.6 M NaOH via an auto-burette to maintain a constant pH in the lipolysis medium at the pre-set value. Blank lipolysis experiments (for micellar solutions) were performed in the same way without the addition of formulation lipids to compensate for the background FFA produced by components other than the studied lipid vehicles. The titrant volume for micelle samples was subtracted from that of the studied lipid formulation samples. The consumption of NaOH (after background correction) was used to calculate the number of moles of FFA liberated based on a 1:1 stoichiometric (acid-base) reaction ratio, which were then used to quantify the magnitude of lipolysis.

The phase distribution of CEL was examined for the SLH microparticles and the blank micelle samples under digesting conditions. At times 1, 5, 15, 30 and 60 min,

aliquots of 1 ml of lipolysis samples were collected into individual Beckman polyallomer tubes prefilled with 10 µl of 4-BPB (0.5 M in methanol) equilibrated at 37°C, which acts as an enzyme inhibitor to stop the lipolysis process in the collected samples. Each collected sample was separated into an upper undigested oil layer, a dispersed aqueous phase and a pellet phase by ultracentrifugation (Beckman XL-80 Ultracentrifuge coupled with a 50 Ti rotor, USA) at 181,000g for 45 min (37°C). The aqueous phase was diluted with acetonitrile (to meet the CEL calibration concentration range) and centrifuged at 1600g for 15 min prior to HPLC analysis as described previously; the pellet fraction was dissolved in a chloroform:methanol (2:1 v/v) mixture and acidified with 100 µl of 1 M HCl prior to the same dilution and centrifugation steps, followed by HPLC analysis. It is noted that isolation of the undigested oil film was not practically feasible due to the low oil content of <10 mg per ml of the collected digestion sample; therefore, the drug content in the oil phase was not determined.

In Vivo Dose-Dependent Absorption Study

Animal Procedures and Formulation Administration

All animal experiments were approved by the Animal Ethics Committee, Institute of Medical and Veterinary Science, IMVS (Australia). Groups of five healthy male Sprague-Dawley rats weighing from 300 to 360 g were used for each treatment in the single oral dose study. One to two days prior to CEL dosing, each rat was cannulated in the right jugular vein under inhaled isoflurane and allowed to recover. The rats were fasted overnight (14±1 h) prior to the day of dosing and were given access to food 4 h post-dose. Water was accessible to all treatment groups throughout the study.

The CEL formulations tested at various doses (i.e. 5, 20 and 50 mg/kg) and the corresponding formulation compositions are listed in Table I. Pure CEL powder and the Celebrex[®] powder materials were suspended in 0.25%w/v sodium carboxymethylcellulose by ultrasonication (for 30 min). The CEL-SLH microparticles were redispersed in Milli-Q water by brief vortex-mixing (10–20 s) and hand-held shaking to form suspensions. Each cannulated and fasted rat was administered one of the listed formulations via oral gavage under light inhaled isoflurane. Blood samples (0.2 ml) were collected from the jugular vein at designated time points (i.e. 0, 0.25, 0.5, 1, 2, 3, 4, 6, 8, 10 and 24 h after dosing) and centrifuged at 9,400g for 5 min. Each aliquot of 100 µl plasma was vortex-mixed with 100 µl acetonitrile and centrifuged at 3,500g for 10 min to remove proteins, prior to HPLC analysis as described before. CEL content in the plasma samples was computed from the same calibration curve (CEL in mobile phase) due

Table 1 The Compositions of CEL Formulations Tested in Rats ($n = 5$ Unless Otherwise Specified)

CEL formulation	Compositions (mg) ^d		Total powder mass administered (mg) ^d	Total volume administered (ml)
	CEL	Lipid		
Low dose: 5 mg/kg ^b				
Pure CEL	1.75	–	1.75	1.75
Celebrex [®]	1.75	–	4.7	2
SLH-M-1	1.75	168	324	2
Medium dose: 20 mg/kg ^c				
Pure CEL	7.0	–	7.0	3
Celebrex [®]	7.0	–	18	3
SLH-M-1 ^d	7.0	409	787	3
SLH-M-2	7.0	241	387	3
SLH-C	7.0	111	182	3
High dose: 50 mg/kg ^{c, d}				
Pure CEL	17.5	–	17.5	3
Celebrex [®]	17.5	–	47	3
SLH-C	17.5	278	455	3

^a The total powder mass includes the active drug, lipid excipients (if any) and other non-lipid inactive ingredients; each total mass of powder administered was estimated based on a rat weighing 350 g.

^b The rats used for the low dose experiments were supplied by the IMVS.

^c The rats used for the medium and high dose experiments were supplied by the Lab Animal Services, University of Adelaide.

^d $n = 4$.

to high extraction recovery (~100%) of CEL from rat plasma samples.

Pharmacokinetic and Statistical Analyses

The CEL plasma concentration (C_p) values obtained were dose-normalised to 5, 20 and 50 mg/kg accordingly in order to eliminate minor dose discrepancies and facilitate comparison between rats. The mean C_p -time curves were constructed based on the mean dose-normalised data. The pharmacokinetic parameters were determined using the PC software, WinNonlin[®] Standard Edition Version 4.1 (Pharsight Corporation, CA), based on a non-compartmental model. The maximum plasma concentration (C_{max}) and the time at which C_{max} is reached (t_{max}) were obtained from the individual C_p -time profiles. The area under the C_p -time curve from time zero to infinity ($AUC_{0 \rightarrow \infty}$), calculated using the linear trapezoidal rule, was used to estimate the relative bioavailability ($F_{rel.}$) of the test formulations with reference to that of the pure CEL, according to Eq. 1 (26):

$$F_{rel.} = \frac{AUC_{0 \rightarrow \infty}(\text{test})}{AUC_{0 \rightarrow \infty}(\text{reference})} \times \frac{\text{Dose (reference)}}{\text{Dose (test)}} \quad (1)$$

All values are expressed as the mean \pm standard error of the mean (SEM). The pharmacokinetic data were evaluated by one-way analysis of variance (ANOVA) with a Least Significant Difference (LSD) post-hoc test using the statistical package for social sciences (SPSS version 15.0) software, with the level of significance set at $p < 0.05$.

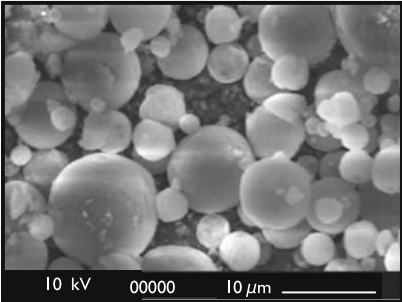
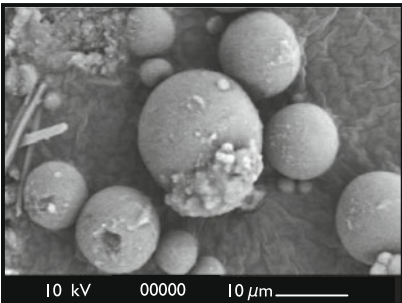
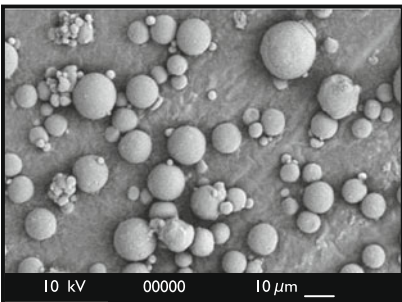
RESULTS

Physicochemical Properties of CEL-SLH Microparticles

Three types of SLH microparticles with varying CEL loading levels were fabricated: SLH-M-1 (0.6% CEL), SLH-M-2 (1.8% CEL) and SLH-C (3.8% CEL) (Table II). Each SLH formulation is comprised of 52 to 62% (w/w) of lipids encapsulated by or embedded in a porous silica-based matrix at an oil:silica mass ratio of approximately 1:0.5 (w/w). The SLH-M-2 formulation is essentially similar to the SLH-M-1 formulation in their compositions except for a higher lecithin level, i.e. oil:lecithin mass ratio of 1:0.5 vs. 1:0.06. This renders an increased CEL loading level in the SLH-M-2 system, as lecithin tends to self-assemble into reversed spherical micellar structures in non-aqueous media (27), thereby improving the solubility of CEL in Miglyol oil. SLH-C contains the highest CEL loading level, mainly due to the higher CEL intrinsic solubility in Capmul MCM, which is an amphiphilic lipid widely used as a surfactant/ emulsifier for oil-water systems (28–30).

The CEL-SLH microparticles were compared in terms of solid-state morphology and redispersed-state colloidal properties as a key indicator of the formulation stability. The CEL-SLH formulations were readily redispersible in water and demonstrated excellent physicochemical stability (CEL in non-crystalline state as shown by XRD) at ambient conditions for a study period of at least 6 months (Fig. 1). Microscopic observation by SEM shows that the SLH microparticles prepared from either Miglyol 812 (i.e. SLH-M-1 and SLH-M-2) or Capmul MCM (i.e. SLH-C)

Table II Physicochemical Properties of Various CEL-SLH Microcapsules Fabricated from Medium-Chain Lipids: Lipid and CEL Content, Solid State Surface Morphology, Redispersed Particle Size and Zeta Potential (Mean \pm S.E.M., $n=3$)

Formulation	Solid state SEM images	Colloidal properties (in water)																					
SLH-M-1 Composition: Lipid ^a 52.0 \pm 0.0% Silica ^b 47.4% CEL 0.6 \pm 0.0%		<table border="1"> <thead> <tr> <th>Size (μm)</th> <th>1 month</th> <th>12 months</th> </tr> </thead> <tbody> <tr> <td>D(v,0.1)</td> <td>0.136 \pm 0.0</td> <td>0.138 \pm 0.0</td> </tr> <tr> <td>D(v,0.5)</td> <td>0.842 \pm 0.0</td> <td>0.802 \pm 0.1</td> </tr> <tr> <td>D(v,0.9)</td> <td>2.896 \pm 0.0</td> <td>3.536 \pm 0.3</td> </tr> <tr> <td>Span</td> <td>3.28 \pm 0.0</td> <td>4.32 \pm 0.6</td> </tr> <tr> <th>ζ (mV)</th> <th>1 month</th> <th>12 months</th> </tr> <tr> <td>Average</td> <td>-67.5 \pm 12.1</td> <td>-80.1 \pm 6.0</td> </tr> </tbody> </table>	Size (μm)	1 month	12 months	D(v,0.1)	0.136 \pm 0.0	0.138 \pm 0.0	D(v,0.5)	0.842 \pm 0.0	0.802 \pm 0.1	D(v,0.9)	2.896 \pm 0.0	3.536 \pm 0.3	Span	3.28 \pm 0.0	4.32 \pm 0.6	ζ (mV)	1 month	12 months	Average	-67.5 \pm 12.1	-80.1 \pm 6.0
Size (μm)	1 month	12 months																					
D(v,0.1)	0.136 \pm 0.0	0.138 \pm 0.0																					
D(v,0.5)	0.842 \pm 0.0	0.802 \pm 0.1																					
D(v,0.9)	2.896 \pm 0.0	3.536 \pm 0.3																					
Span	3.28 \pm 0.0	4.32 \pm 0.6																					
ζ (mV)	1 month	12 months																					
Average	-67.5 \pm 12.1	-80.1 \pm 6.0																					
SLH-M-2 Composition: Lipid ^c 62.3 \pm 0.2% Silica ^b 35.9% CEL 1.8 \pm 0.1%		<table border="1"> <thead> <tr> <th>Size (μm)</th> <th>1 month</th> <th>6 months</th> </tr> </thead> <tbody> <tr> <td>D(v,0.1)</td> <td>0.107 \pm 0.0</td> <td>0.106 \pm 0.0</td> </tr> <tr> <td>D(v,0.5)</td> <td>0.616 \pm 0.0</td> <td>0.485 \pm 0.0</td> </tr> <tr> <td>D(v,0.9)</td> <td>3.989 \pm 0.0</td> <td>2.584 \pm 0.1</td> </tr> <tr> <td>Span</td> <td>6.30 \pm 0.1</td> <td>5.26 \pm 0.1</td> </tr> <tr> <th>ζ (mV)</th> <th>1 month</th> <th>6 months</th> </tr> <tr> <td>Average</td> <td>-68.6 \pm 3.8</td> <td>-73.1 \pm 1.0</td> </tr> </tbody> </table>	Size (μm)	1 month	6 months	D(v,0.1)	0.107 \pm 0.0	0.106 \pm 0.0	D(v,0.5)	0.616 \pm 0.0	0.485 \pm 0.0	D(v,0.9)	3.989 \pm 0.0	2.584 \pm 0.1	Span	6.30 \pm 0.1	5.26 \pm 0.1	ζ (mV)	1 month	6 months	Average	-68.6 \pm 3.8	-73.1 \pm 1.0
Size (μm)	1 month	6 months																					
D(v,0.1)	0.107 \pm 0.0	0.106 \pm 0.0																					
D(v,0.5)	0.616 \pm 0.0	0.485 \pm 0.0																					
D(v,0.9)	3.989 \pm 0.0	2.584 \pm 0.1																					
Span	6.30 \pm 0.1	5.26 \pm 0.1																					
ζ (mV)	1 month	6 months																					
Average	-68.6 \pm 3.8	-73.1 \pm 1.0																					
SLH-C Composition: Lipid ^a 61.0 \pm 0.0% Silica ^b 35.2% CEL 3.8 \pm 0.0%		<table border="1"> <thead> <tr> <th>Size (μm)</th> <th>1 month</th> <th>6 months</th> </tr> </thead> <tbody> <tr> <td>D(v,0.1)</td> <td>0.133 \pm 0.0</td> <td>0.131 \pm 0.0</td> </tr> <tr> <td>D(v,0.5)</td> <td>0.696 \pm 0.0</td> <td>0.575 \pm 0.0</td> </tr> <tr> <td>D(v,0.9)</td> <td>5.665 \pm 0.2</td> <td>4.072 \pm 0.4</td> </tr> <tr> <td>Span</td> <td>7.94 \pm 0.2</td> <td>6.82 \pm 0.4</td> </tr> <tr> <th>ζ (mV)</th> <th>1 month</th> <th>6 months</th> </tr> <tr> <td>Average</td> <td>-83.1 \pm 13.7</td> <td>-77.7 \pm 3.4</td> </tr> </tbody> </table>	Size (μm)	1 month	6 months	D(v,0.1)	0.133 \pm 0.0	0.131 \pm 0.0	D(v,0.5)	0.696 \pm 0.0	0.575 \pm 0.0	D(v,0.9)	5.665 \pm 0.2	4.072 \pm 0.4	Span	7.94 \pm 0.2	6.82 \pm 0.4	ζ (mV)	1 month	6 months	Average	-83.1 \pm 13.7	-77.7 \pm 3.4
Size (μm)	1 month	6 months																					
D(v,0.1)	0.133 \pm 0.0	0.131 \pm 0.0																					
D(v,0.5)	0.696 \pm 0.0	0.575 \pm 0.0																					
D(v,0.9)	5.665 \pm 0.2	4.072 \pm 0.4																					
Span	7.94 \pm 0.2	6.82 \pm 0.4																					
ζ (mV)	1 month	6 months																					
Average	-83.1 \pm 13.7	-77.7 \pm 3.4																					

^a The lipid content refers to a oil:lecithin mass ratio of 1:0.06.

^b The content of silica is an estimation resulting from subtraction of the content of lipid and CEL.

^c The lipid content refers to a oil:lecithin mass ratio of 1:0.5.

consist of well-separated spherical structures with heterogeneous size distributions ranging from 1 to 15 μm in the solid state (Table II). Particle sizing by laser diffraction indicates a relatively larger $D(v,0.9)$ value for Capmul-based microparticles (4–5 μm) compared to that of Miglyol-based microparticles (2–4 μm), yet the $D(v,0.1)$ and $D(v,0.5)$ diameters are comparable for all formulations ($<1 \mu\text{m}$). The time-dependent changes in the particle sizes are considered to be modest for the SLH microparticle systems examined in this study. Importantly, the presence of particles larger than 10 μm was confirmed to be negligible in all types of microparticle systems. The zeta potentials (ζ) of the anionic emulsion systems remained at $>40 \text{ mV}$ in magnitude before and

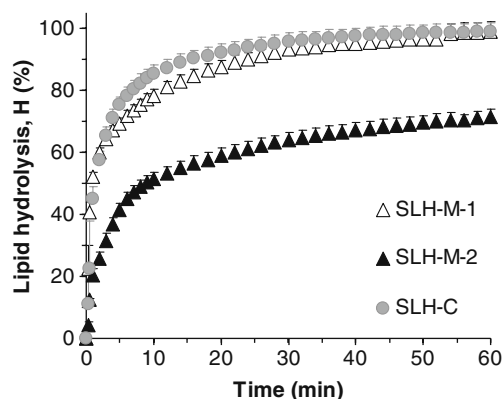


Fig. 2 Time dependence of the enzyme-mediated lipolysis for various CEL-SLH microparticles under simulated fasted intestinal conditions at 37°C (mean \pm S.E.M., $n=3$).

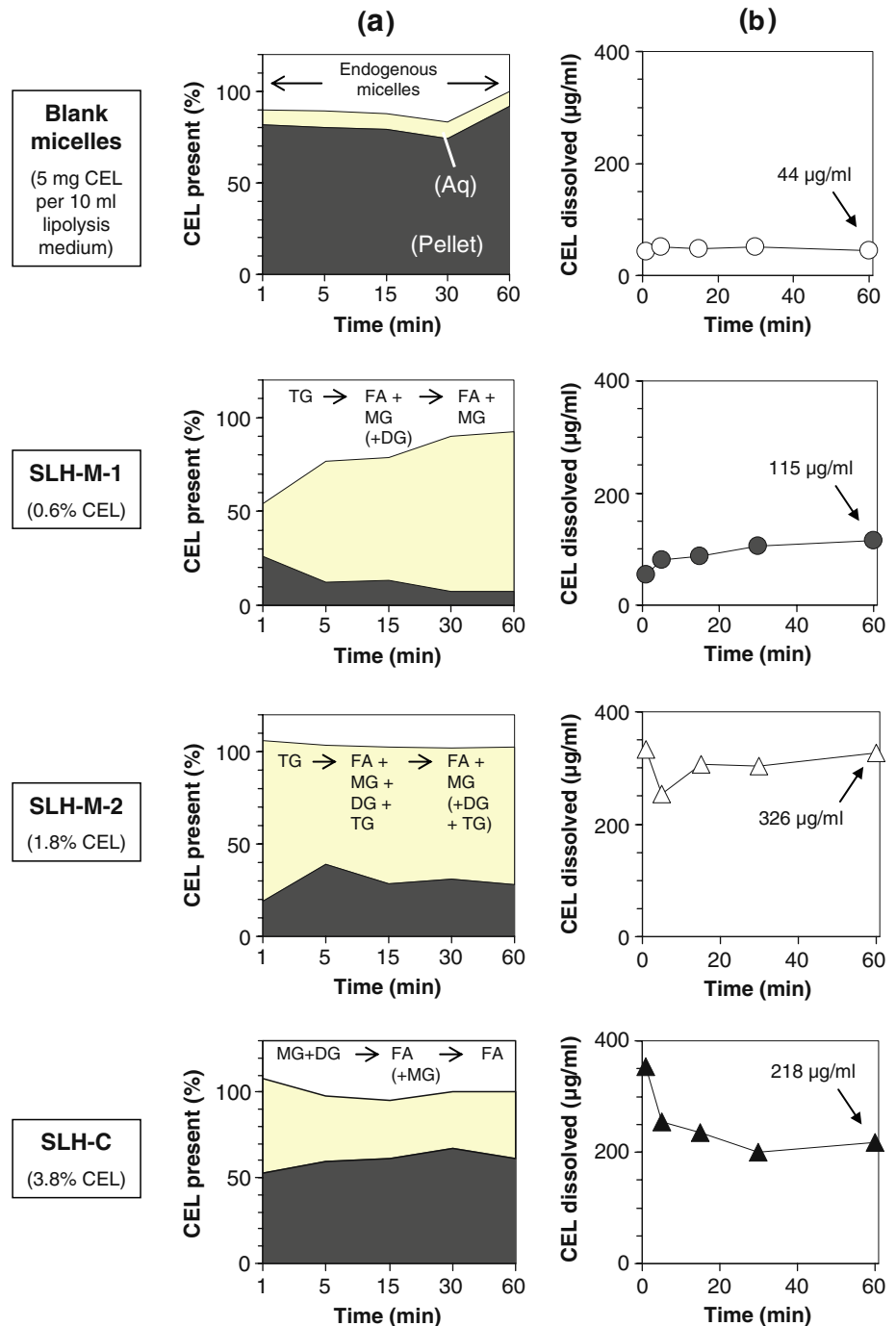
after spray-drying. Taken together, the SLH microparticles showed reproducible reconstitution properties in simulated intestinal medium (pH 7.2).

In Vitro Solubilisation of CEL Under Digesting Conditions

Lipolysis-time profiles for the CEL-SLH microparticles are presented in Fig. 2. SLH-M-1 and SLH-C formulations,

which contain low levels of lecithin, produced a relatively faster and more complete lipolysis (~100% at 60 min) than the SLH-M-2 formulation, which contains a higher level of lecithin (~70% lipolysis at 60 min). This highlights the inhibitory role of lecithin on the digestion of mixed glyceride-lecithin systems where lecithin presumably forms a competitive binding site for the lipid-digesting enzymes, thereby reducing the accessibility of enzymes to the glyceride components during lipolysis (31).

Fig. 3 Phase distribution of CEL in the simulated fasted state intestinal medium (5 mM bile salt: 1.25 mM phospholipid) at 37°C ($n = 2$): **(a)** percentage of CEL distributed in the aqueous and pellet phases, and the likely species of lipid products generated (36), and **(b)** concentration of CEL solubilised in the lipolysis aqueous phase.



The percentage of CEL present in the aqueous and pellet phases during lipolysis (Fig. 3a) shows that continuous lipolysis of the SLH microparticles provides a significantly higher solubilising environment for CEL (30–100% CEL solubilised) in comparison to the fasted-state blank micellar solution (<10% CEL solubilised). In this study, the lipid dose was fixed at 10 mg/ml in the lipolysis medium; this corresponds to a maximum achievable CEL concentration of approximately 100 µg/ml, 370 µg/ml and 620 µg/ml for SLH-M-1, SLH-M-2 and SLH-C, respectively. The partition results (Fig. 3a) show that there is a higher percentage of CEL solubilised into the aqueous phase than precipitated for both types of Miglyol-based microparticle systems, but there is a higher tendency of drug precipitation than solubilisation for the Capmul-based microparticles, most probably due to the much higher CEL dose in the latter case. Therefore, it is more appropriate to compare the solubilisation results in terms of the absolute concentrations (Fig. 3b) rather than the percentage of CEL solubilised.

Based on the lipolysis-time profile in Fig. 2, a complete lipolysis of a 10 mg/ml lipid dose could produce a final solubilised CEL concentration of 115 µg/ml for SLH-M-1, which is approximately 2.5-fold higher than that of the blank micelle medium (44 µg/ml) and 16-fold greater than the solubility of CEL in water (i.e. 7 µg/ml (32)). When compared to the SLH-M-2 microparticles, even though the lipid digestion was slower and incomplete (~70% lipolysis at 60 min), the solubilisation curve (Fig. 3b) reveals a significantly higher concentration of CEL dissolved ranging from 250 to 330 µg/ml. Whilst the equilibrium solubility of CEL in Capmul MCM (9.3%) was determined to be significantly higher than that in Miglyol oil (1.1%), the lipolytic products of SLH-C microparticles were found to provide less solubilising capacity than the SLH-M-2 system, as evidenced by a lower concentration of CEL solubilised (218 µg/ml) after a complete lipolysis. The *in vitro* AUC values of CEL

solubilised in the lipolysis aqueous phase, derived from the drug solubilisation curve (Fig. 3b), are summarised in Table III. These *in vitro* AUC values are used for developing correlations with the *in vivo* AUC values in the later section on *in vitro-in vivo* correlations.

In Vivo Absorption of Various Celecoxib Formulations

The dose-dependent absorption of CEL was systematically evaluated for various oral formulations at three dosage levels (i.e. 5, 20 and 50 mg/kg CEL) in a fasted rat model. The formulations of interest include pure CEL, Celebrex[®] capsule materials and the CEL-SLH microparticles, all dosed in the form of an aqueous suspension. The mean C_p -time profile of each studied formulation is presented in Fig. 4. The corresponding non-compartmental pharmacokinetic data are summarised in Table IV.

At the lowest dose level of 5 mg/kg CEL, pure CEL produced the lowest C_{max} and $AUC_{0 \rightarrow \infty}$ values among the tested formulations. A modest (but not statistically significant) improvement in the bioavailability was observed for the suspended Celebrex[®] materials, which showed an increased C_{max} and $F_{rel.}$ (133%) in comparison with pure CEL. Interestingly, SLH-M-1 exhibited a statistically higher C_{max} and $F_{rel.}$ (150%) as compared to pure CEL ($p < 0.05$). The t_{max} values remained constant (i.e. 2–3 h) across the various treatment groups.

When CEL was administered at higher doses (i.e. 20–50 mg/kg), both Celebrex[®] and the CEL-SLH formulations exhibited a 2–2.5-fold higher bioavailability (i.e. $F_{rel.} = 191–244\%$) compared to pure CEL ($p < 0.05$). Considering that the bioavailability is comparable between SLH-M-1, SLH-M-2 and SLH-C at the dose of 20 mg/kg, as well as a reasonable total feed dose size (i.e. total mass of administration <1 g per rat), the ‘high dose’ experiments conducted at 50 mg/kg CEL were undertaken for the SLH-C formulation because of its higher CEL loading level and, hence, lower mass of administration required. From Table IV, the pharmacokinetic data indicate that SLH-C is capable of increasing the absorption of CEL at both medium and high doses, in which the absorption profiles are comparable to that of the suspended Celebrex[®] materials.

In order to clearly illustrate the dose-pharmacokinetic relationships, the values of $AUC_{0 \rightarrow \infty}$ and C_{max} obtained for pure CEL, Celebrex[®] and the CEL-SLH microparticles are plotted against the dose of CEL administered (Fig. 5). The formulations of SLH-M-1, SLH-M-2 and SLH-C were regarded as the same treatment group because only subtle differences have been observed in their bioavailability. Interestingly, the $AUC_{0 \rightarrow \infty}$ and C_{max} values increase linearly with the selected CEL doses (i.e. 5,

Table III The Values of Area-Under-the Curve (with the Number of Fold of Increment Compared to Blank Micelles) Derived from the CEL Solubilisation Plots for Various CEL Formulations During Digestion Under Fasted-State Intestinal Conditions at 37°C ($n = 2$)

Lipid systems	$AUC_{1 \rightarrow t}$ (min.mg/ml) ^a			
	$t = 5$ min	$t = 15$ min	$t = 30$ min	$t = 60$ min
Blank micelles	0.190	0.688	1.43	2.84
SLH-M-1	0.270 (1.4)	1.11 (1.6)	2.55 (1.8)	5.87 (2.1)
SLH-M-2	1.17 (6.2)	3.98 (5.8)	8.56 (6.0)	18.0 (6.3)
SLH-C	1.22 (6.4)	3.66 (5.3)	6.91 (4.8)	13.2 (4.6)

^a The standard deviations of the reported mean values are less than 2%

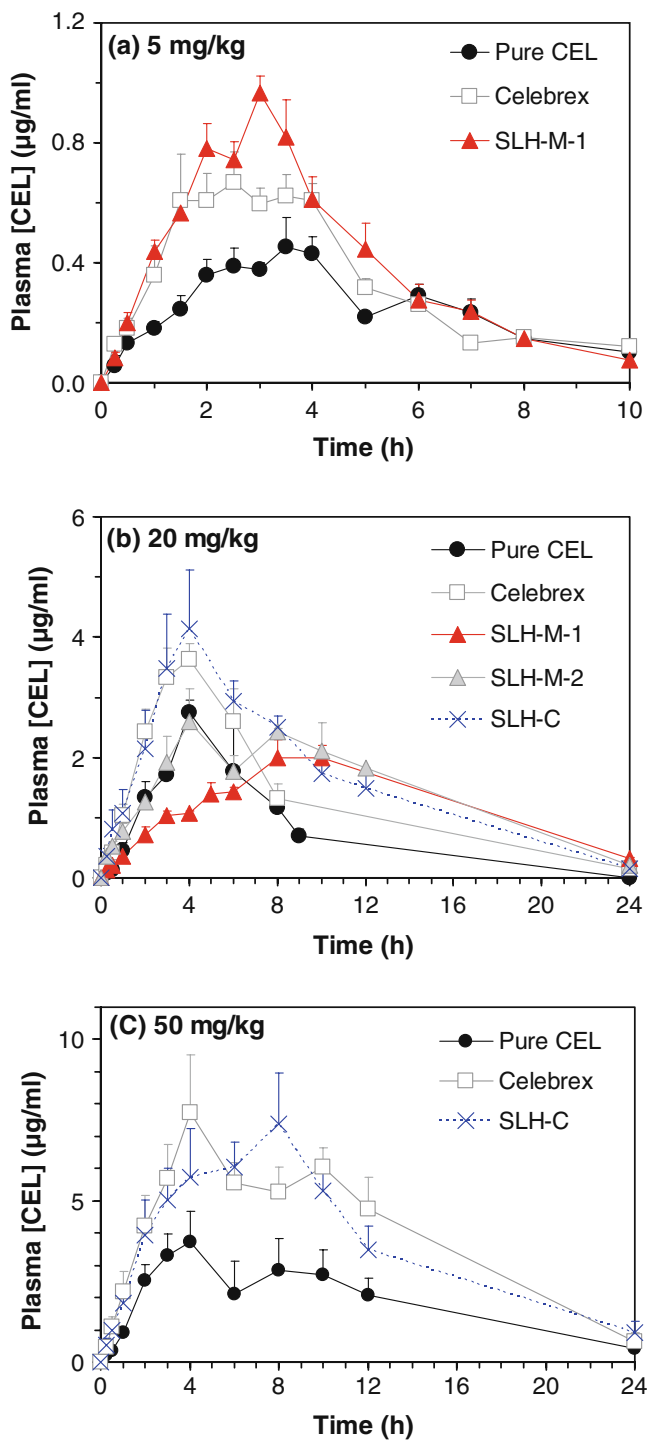


Fig. 4 Plasma concentration-time profiles of CEL in fasted, male Sprague-Dawley rats following a single oral dose of various formulations equivalent to a CEL dose of (a) 5 mg/kg ($n = 5$), (b) 20 mg/kg ($n = 5$), and (c) 50 mg/kg ($n = 4$) (mean \pm S.E.M.).

20 and 50 mg/kg) for all three studied formulations. The dose-pharmacokinetic relationships are reasonably linear in all scenarios ($R^2 \geq 0.99$), except for the C_{max} increment for pure CEL ($R^2 = 0.82$).

In Vitro-In Vivo Correlations (IVIVC)

Single-Point Correlations

Single-point correlations were established to rank the *in vivo* performance of the studied CEL formulations (regardless of the statistical significance of bioavailability data). Correlations were established using the *in vitro* CEL solubilisation data and the pharmacokinetic results obtained at a CEL dose of 20 mg/kg, considering that the amount of CEL administered to the rats (i.e. 6–7.2 mg CEL per rat) is within the range of the CEL dose incorporated into the *in vitro* lipolysis studies (i.e. 2–12.4 mg CEL in a 20 ml lipolysis medium). The *in vivo* $AUC_{0 \rightarrow \infty}$ or C_{max} values were correlated with (i) the final concentration of CEL solubilised in the post-lipolysis aqueous phase at 60 min, i.e. $[CEL]_{aq(60 \text{ min})}$ and (ii) the maximum concentration of CEL solubilised in the aqueous phase during lipolysis, i.e. $[CEL]_{aq(max)}$. Fig. 6a and b clearly depict a linear IVIVC for pure CEL, SLH-M-1 and SLH-M-2 ($R^2 > 0.9$ with a zero intercept), in which case the $[CEL]_{aq}$ in the post-digestive state (i.e. after 60 min of lipolysis) was considered. However, SLH-C was not fitted into the correlations. On the other hand, when the values of $[CEL]_{aq(max)}$ were taken to correlate with the $AUC_{0 \rightarrow \infty}$ or C_{max} values, a strong correlation was obtained between these parameters for all four studied formulations: pure CEL < SLH-M-1 < SLH-M-1 < SLH-C ($R^2 > 0.9$ with a zero intercept in both plots) (Fig. 6c and d).

Multiple-Point Correlations

Multiple-point correlations were established for each formulation based on the *in vitro* AUC values of drug solubilised in the lipolysis aqueous phase and the *in vivo* AUC values derived from the C_p -time profiles at various time points (for rats dosed at a 20 mg/kg CEL dose). Specifically, the percentage of lipolysis at time ($t_{in vitro}$) = 1, 5, 15, 30, and 60 min was correlated with the plasma concentration of CEL determined at time ($t_{in vivo}$) = 15, 30, 60, 120, and 180 min, when the absorption rate was greater than the elimination rate (i.e. at times prior to reaching C_{max}). As depicted in Fig. 7, linear IVIVCs were obtained for pure CEL (in the absence of formulation lipids), SLH-M-1, SLH-M-2 and SLH-C ($R^2 > 0.9$ with a zero intercept). When the selected time points for both *in vitro* and *in vivo* data are plotted against one another according to the concept of a Levy plot (i.e. $t_{in vivo}$ vs. $t_{in vitro}$) (33), it yields a slope of approximately three (Fig. 8). This slope value can be used to infer that the *in vivo* absorption occurs three-fold slower than the *in vitro* lipolysis under the simulated intestinal conditions.

Table IV Dose-Dependent Pharmacokinetic Parameters of CEL Following a Single Oral Dose of Various CEL Formulations to Fasted, Male Sprague-Dawley Rats Based on Non-Compartmental Calculation (Mean \pm S.E.M., $n=5$ Unless Otherwise Specified)

CEL formulation	Pharmacokinetic parameters			
	t_{\max} (min)	C_{\max} ($\mu\text{g/ml}$)	$AUC_{0\rightarrow\infty}$ (min, $\mu\text{g/ml}$)	F_{rel} (%)
Low dose: 5 mg/kg				
Pure CEL	202 \pm 28	0.50 \pm 0.08	167 \pm 11	100 \pm 7
Celebrex [®]	162 \pm 20	0.63 \pm 0.08	223 \pm 16	133 \pm 9
SLH-M-1	174 \pm 15	1.00 \pm 0.07 ^{a, b}	250 \pm 15 ^a	150 \pm 9 ^a
Medium dose: 20 mg/kg				
Pure CEL	270 \pm 30	2.92 \pm 0.37	951 \pm 153	100 \pm 16
Celebrex [®]	252 \pm 29	4.18 \pm 0.28	1882 \pm 177 ^a	198 \pm 19 ^a
SLH-M-1*	560 \pm 40 ^{a, b}	2.16 \pm 0.29	1859 \pm 109 ^a	195 \pm 12 ^a
SLH-M-2	456 \pm 59 ^{a, b}	3.21 \pm 0.44	2036 \pm 187 ^a	214 \pm 20 ^a
SLH-C	264 \pm 24	4.33 \pm 0.89	2316 \pm 259 ^a	244 \pm 27 ^a
High dose: 50 mg/kg				
Pure CEL*	285 \pm 66	3.88 \pm 0.96	3089 \pm 546	100 \pm 18
Celebrex [®] *	300 \pm 60	8.83 \pm 0.85 ^a	5975 \pm 525 ^a	193 \pm 17 ^a
SLH-C*	360 \pm 69	9.10 \pm 0.74 ^a	5895 \pm 565 ^a	191 \pm 18 ^a

* $n=4$

^a statistically higher than aqueous suspension ($p < 0.05$)

^b statistically higher than Celebrex[®] ($p < 0.05$)

DISCUSSION

Solubilisation of CEL from Post-Digested SLH Microparticles

SLH microparticles, originated from oil-in-water emulsion templates, were formulated based on medium-chain glycerides (either TG or a MG/DG blend) as the oil phase, soybean lecithin as the emulsifier, and Aerosil silica nanoparticles as the stabiliser and solid carrier, all of which are GRAS-listed substances. The formation of macro-porous (50–200 nm), homogenous silica-lipid matrices has been illustrated by a previous ion beam-induced SEM analysis (15,34). The highly porous matrix structure of the SLH microparticles (BET surface area=184 m²/g) has been shown to contribute towards an enhanced lipid digestibility and, hence, *in vivo* drug bioavailability as compared to conventional lipid solutions and submicron emulsions (34). Significantly, the current study provides a full characterisation of the dynamic solubilisation state of the encapsulated drugs before, during, and after enzymatic digestion of the SLH microparticles.

A parallel analysis of the lipolysis kinetics and drug phase partitions provides an important insight into the mechanisms of drug release and solubilisation resulting from the SLH microparticle systems. The lipolysis profiles show that the nano-structured SLH microparticles are effective in enhancing complete digestion of Miglyol 812 (TG) and Capmul MCM (MG/DG blend) in the presence of low lecithin levels (oil:lecithin=1:0.06 w/w). Interestingly, lecithin has played a dual role in the formulation of SLH microparticles—it acts as a solubiliser (or termed ‘biosurfactant’ (35)) for improving the lipid solubility of CEL but, on the other hand, exerts an inhibitory effect on the digestion of lipid oils. This is an

attractive mechanism in which the inhibitory role of lecithin dominates the positive porosity effect of the SLH microparticle systems in producing a more controllable rate and extent of lipolysis.

To verify the role of lipid digestibility on drug solubilisation, the distribution of CEL between the aqueous and pellet phases during lipid digestion was determined for CEL in blank micelles (without the addition of exogenous lipids), as well as for various SLH formulations. The lipolysis phase partition data indicate a 2.5–7.5-fold higher solubilising capacity in the lipolysis medium resulting from the digestion of SLH microparticles encapsulating the medium-chain lipids, as compared to the simulated fasted-state endogenous micelles. The initial solubility of the CEL in the lipid vehicles does not directly correlate to the medium solubilisation capacity after lipolysis. It is proposed that the types of the end lipolysis products, either in the partially digested but absorbable forms (i.e. MG and DG) or in the completely hydrolysed and titratable form (i.e. FFA), significantly influence the solubilising power of a lipolysis medium. According to one of the original papers describing the lipolysis model developed by Sek *et al.* (36), medium-chain TG is expected to be hydrolysed to form MG (15%) and FA (70%) in the aqueous phase, with some FA (15%) pelleted out after 30 min; DG is also possibly accumulated in the first 5 min of lipolysis. In contrast, medium-chain MG/DG mixture is completely hydrolysed in 30 min to produce only FA as the end products, in which 80% is present in the aqueous phase and the remaining 20% in the pellet phase. Based on this information, we deduced that the partially digested glyceride forms, specifically MG and DG, are important solubilising colloidal species that prevent precipitation of the unionised CEL molecules. Full lipid hydrolysis may not be necessary to

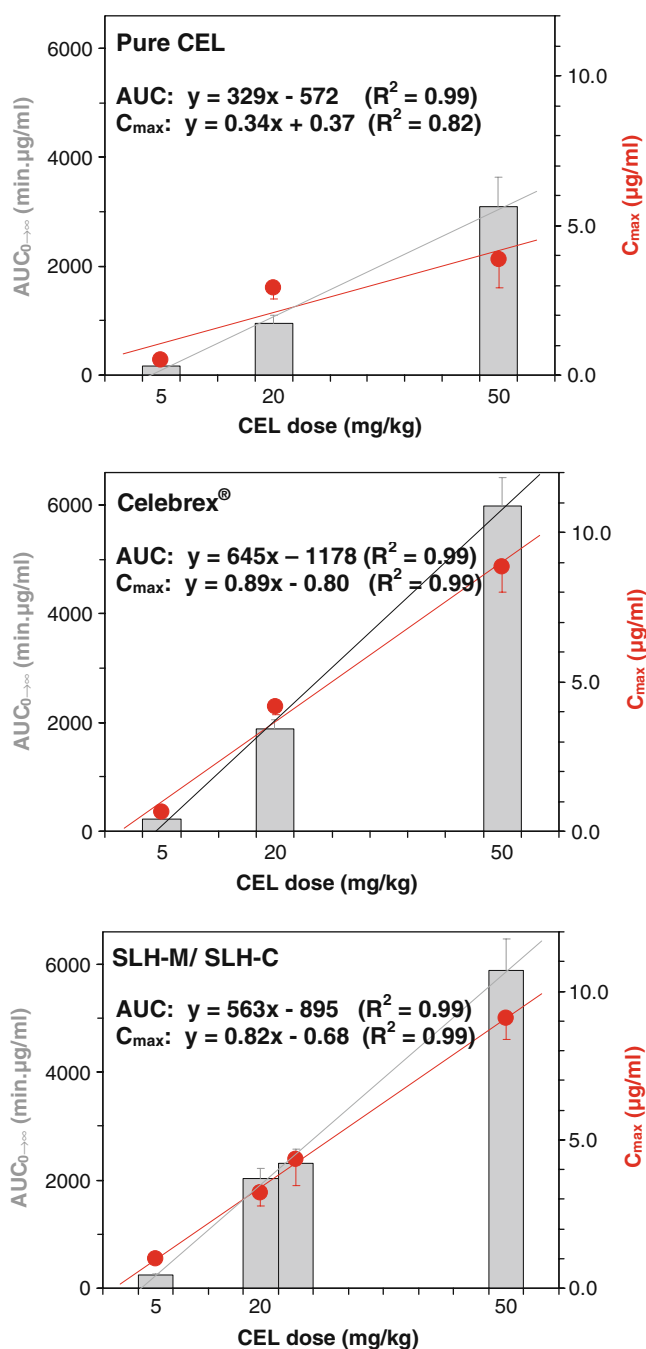


Fig. 5 Linearity in pharmacokinetics of CEL over the dose range of 5–50 mg/kg following a single oral administration of various CEL formulations to fasted, male Sprague-Dawley rats: $AUC_{0 \rightarrow \infty}$ (grey bars) and C_{max} (closed circles).

induce drug release and solubilisation. This inherently elucidates the higher initial concentration of CEL solubilised for the SLH-C system because of the presence of a MG/DG mixture. As lipolysis progresses, the concentration of the MG/DG species declines rapidly because they are efficiently digested by the lipase/colipase complexes, producing the titratable FFA monomers which do not favour solubilisation of the CEL

molecules. Hence, a declining solubilisation curve was observed for the SLH-C microparticles under digesting conditions. In the case of SLH-M-2 microparticles, the continuous gain of the MG and DG species with incomplete conversion into the titratable FFA has adequately maintained CEL dispersion in the lipolysis aqueous phase.

Dose-Dependent Absorption of CEL

The dose-dependent absorption profiles of CEL resulting from various oral formulations were determined in a fasted rat model: pure CEL, Celebrex[®] (which is ‘surfactant-based’ (1)) and the lipid-based SLH microparticle systems. The lowest CEL dose employed (i.e. 5 mg/kg) is equivalent to the efficacious anti-inflammatory dose of 400 mg daily in humans, assuming an average weight of 70–80 kg; the higher doses employed (i.e. 20 and 50 mg/kg) are useful for the evaluation of dose-pharmacokinetic linearity as well as for potential translation into anti-cancer uses (37). To date, there have been few studies reporting dose proportionality assessment of CEL when administered in various dosage forms; Mamidi *et al.* (6) have reported linear dose-pharmacokinetic responses in rats for their CEL prodrug formulation, but not for the conventional CEL formulation (suspension) over the dose range of 10–100 mg/kg.

The current single-dose absorption studies have shown reasonably linear dose-pharmacokinetic relationships for both non-lipid (pure CEL and Celebrex[®]) and lipid-based (CEL-SLH microparticles) formulations (Fig. 5). It appears that the R^2 values are close to unity ($R^2=0.99$) except for the C_{max} increment observed for pure CEL ($R^2=0.82$). This is considered to be a result of slower dissolution and absorption taking place in the gut, which subsequently leads to a slower increase in C_{max} for pure CEL at higher doses; surfactant-based and lipid-based formulations have better intraluminal solubilising capacity; therefore, the increment in C_{max} is rather linear within 5–50 mg/kg CEL doses. Since the slope of each plot in Fig. 5 represents the change in $AUC_{0 \rightarrow \infty}$ or C_{max} values as a function of CEL dose, the slope results obtained for Celebrex[®] and the CEL-SLH formulations imply that these formulations consistently provide a two-fold higher CEL bioavailability or C_{max} than pure CEL within the dose range of 5–50 mg/kg. Such bioavailability improvements (i.e. >20%) are regarded as clinically significant (26).

A parallel examination of the SLH-M-1, SLH-M-2 and SLH-C formulations at the same CEL dosage level (*viz.* 20 mg/kg) allows determination of the effect of different lipid dose and lipid type on the absorption of CEL. The mass ratios of lipid:CEL for SLH-M-1, SLH-M-2 and SLH-C are 58:1, 34:1 and 16:1, respectively. From

Fig. 6 Single-point correlations for various CEL formulations including pure CEL (●), SLH-M-1 (▲), SLH-M-2 (▲), and SLH-C (×). The final concentration of CEL solubilised in the post-lipolysis aqueous phase at 60 min ($[\text{CEL}]_{\text{aq}}(60 \text{ min})$) was correlated to (a) the bioavailability ($AUC_{0 \rightarrow \infty}$) and (b) the maximum plasma concentration (C_{max}). The maximum concentration of CEL solubilised in the aqueous phase during lipolysis (i.e. $[\text{CEL}]_{\text{aq}}(\text{max})$) was correlated to (c) $AUC_{0 \rightarrow \infty}$ and (d) C_{max} . Note that in panels a and b, SLH-C is an outlier which is not fitted into the least squares regression lines.

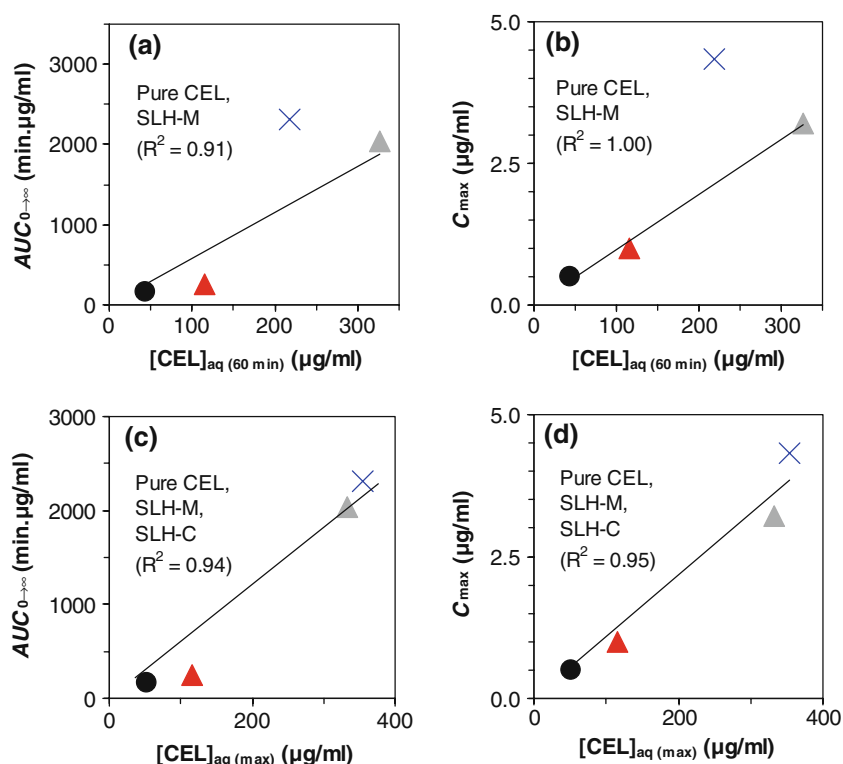
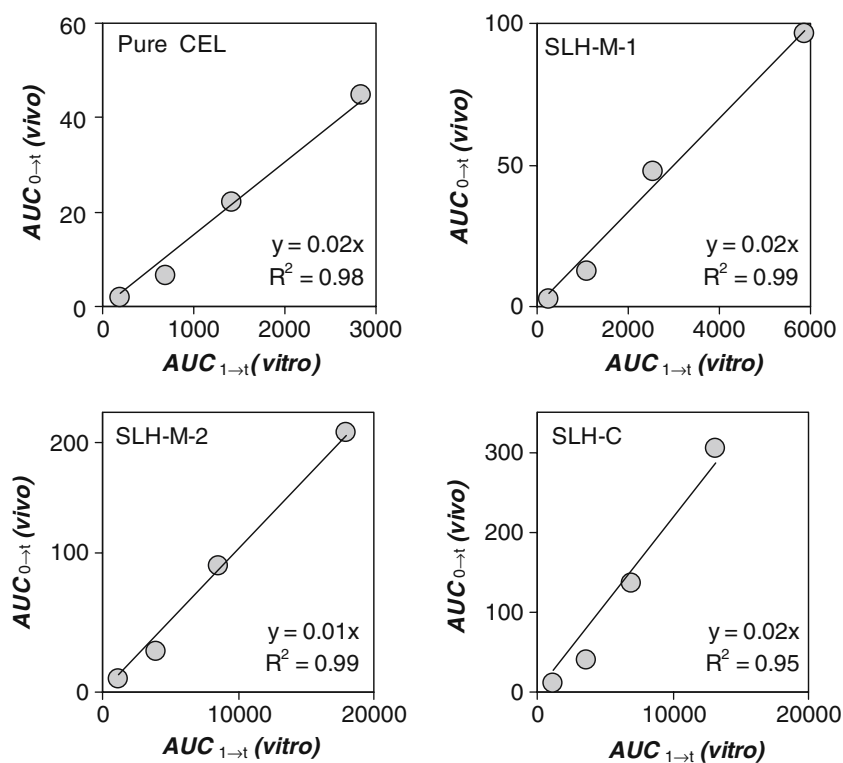


Table IV, it can be seen that both SLH-M-1 and SLH-M-2 formulations produced a significant delay in the absorption process as evidenced by the statistically higher t_{max} values (7–9 h), presumably resulting from the higher lipid

mass of ~400 mg and ~240 mg Miglyol oil administered, respectively (as summarised in Table I). In contrast, SLH-C, which contains ~110 mg Capmul oil per dose, showed a t_{max} value of ~4 h, which is similar to that observed for pure CEL

Fig. 7 Multiple-point correlations between the AUC of CEL solubilised in the *in vitro* lipolysis aqueous phase obtained at $t = 5, 15, 30$ and 60 min, and the *in vivo* AUC data of celecoxib obtained at $t = 30, 60, 120$ and 180 min resulted from oral administration of the corresponding lipid dosage forms. All AUC values are expressed in the unit of $\text{min} \cdot \mu\text{g}/\text{ml}$.



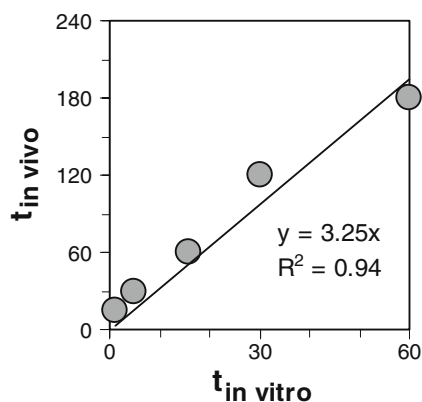


Fig. 8 The time points selected from the *in vivo* absorption study ($t_{in vivo}$) against the time points chosen from the *in vitro* lipolysis study ($t_{in vitro}$) for the development of IVVC (resembling the Levy plot).

and Celebrex[®]. Such findings indicate that co-administration of a high amount of TG (i.e. ≥ 240 mg Miglyol oil in the present case) potentially extends CEL absorption. However, the overall bioavailability of CEL was not affected, in which the $AUC_{0 \rightarrow \infty}$ values of SLH-M-1 and SLH-M-2 are statistically higher than that of pure CEL suspension and comparable to other tested formulations, including Celebrex[®] and SLH-C. Previously, Friedman *et al.* (38) have demonstrated that fat emulsions (e.g. Intralipid) tend to partition in the stomach into an aqueous phase, which empties much faster than the retained oil phase. The delayed/ extended CEL absorption observed for SLH-M-1 and SLH-M-2 may be caused by several mechanisms: (i) a delay in gastric emptying (38), (ii) an extended intestinal transit time (33,39), or (iii) simply a longer digestion time required for the higher amount of lipids prior to drug absorption. It is noted that there is no significant delay in the t_{max} for SLH-C even though the mass of lipid administered is considered high (~ 280 mg MG/DG) at the dose level of 50 mg/kg CEL. The unchanged rate of absorption for the SLH-C formulation may be rationalised by the composition of Capmul oil, which consists primarily of MG (58%) that is readily absorbable across the intestinal membrane, and DG (36%) that hydrolyses quickly into the absorbable forms (MG and FA) (40).

Correlations Between *In Vitro* Solubilisation and *In Vivo* Bioavailability

Our previous work has illustrated the use of lipolysis kinetics to interpret, to some extent, the *in vivo* drug absorption profiles resulting from various lipid-based systems, including simple lipid solutions, emulsions, and SLH microparticles (34). The current phase partition results further elucidate the capability of the resultant digestion products in keeping the

released drugs solubilised during and after lipolysis. It is emphasised that the *in vivo* bioavailability of the tested CEL formulations are more accurately represented by the maximum solubilisation level (i.e. $[CEL]_{aq} (max)$) than the post-lipolysis solubilisation level (i.e. $[CEL]_{aq} (60 \text{ min})$). This correlation approach was developed based on the concept of the drug supersaturation effect as suggested by Guzman *et al.* (23) and Brouwers *et al.* (22). The authors proposed that the creation of a highly supersaturated environment in the GI lumen (even for a limited period of time) is an important mechanism that facilitates the intestinal absorption of highly permeable drugs, such as CEL. The linear correlations obtained between the maximum achievable aqueous solubilisation level in the lipolysis medium and the *in vivo* bioavailability of CEL for all four studied formulations ($R^2 > 0.9$ with a zero intercept in both plots) strongly support the ‘supersaturation’ concept. Time-dependent drug precipitation observed in the *in vitro* lipolysis model may not be reflective of the *in vivo* situation. This argument strongly holds particularly for drugs that are highly permeable to the intestinal membrane, in which the drugs potentially undergo rapid absorption once they are solubilised in a supersaturated state. The correlation approaches reported in this paper represent a significant novelty in the studies of lipolysis-based IVVC and, therefore, will be further investigated in our laboratory using different types of lipid excipients and model lipophilic drugs.

CONCLUSION

The oral absorption profiles of CEL were determined in a dose-dependent manner in a fasted rat model following a single administration of various non-lipid (pure CEL and Celebrex[®]) and lipid-based formulations (SLH microparticles encapsulating medium-chain lipids). Dose linearity in the $AUC_{0 \rightarrow \infty}$ and C_{max} values ($R^2 = 0.82\text{--}0.99$) was confirmed for all three studied formulations at CEL dose levels of 5, 20 and 50 mg/kg. The CEL-SLH formulations and Celebrex[®] consistently produced 2-fold higher $AUC_{0 \rightarrow \infty}$ and C_{max} values than the pure drug within the dose range of 5–50 mg/kg CEL. A parallel analysis of the *in vitro* lipolysis kinetics and drug phase partitions reveals that glycerides in the partially digested forms (i.e. MG and probably DG), rather than the completely hydrolysed form (i.e. FFA), are the important colloidal species determining the solubilising power of a lipolysis medium for CEL. The improved oral absorption of CEL delivered using the SLH microparticles is likely to be facilitated by an enhanced lipid digestibility and subsequent supersaturated solubilisation of CEL by the partially digested but absorbable glyceride species, which eventually leads to an enhanced bioavailability of the highly permeable drug molecules.

ACKNOWLEDGMENTS

The authors would like to thank Miss Kathy Lee (Monash Institute of Pharmaceutical Sciences) for technical support on the lipolysis work and Dr. Mihail Popescu (Ian Wark Research Institute) for useful discussion. Financial support of the Australian Research Council, Bio Innovation SA and Itek Pty. Ltd. are also gratefully acknowledged.

REFERENCES

- US Food and Drug Administration. Celebrex[®] (celecoxib) capsules; 1998 December 31. Available from <http://www.fda.gov/cder/foi/label/2005/020998s018,019lbl.pdf>.
- US Food and Drug Administration. COX-2 selective (includes Bextra, Celebrex, and Vioxx) and non-selective non-steroidal anti-inflammatory drugs (NSAIDs); 2005 July 4. Available from <http://www.fda.gov/Drugs/DrugSafety/PostmarketDrugSafetyInformationforPatientsandProviders/ucm103420.htm>.
- Australian Therapeutic Goods Administration. Medicines Regulator cancels registration of anti-inflammatory drug, Lumiracoxib (Prexige); 2007 August 11. Available from <http://www.tga.gov.au/media/2007/070811-lumiracoxib.htm>.
- Paulson SK, Vaughn MB, Jessen SM, Lawal Y, Gresk CJ, Yan B, *et al.* Pharmacokinetics of celecoxib after oral administration in dogs and humans: effect of food and site of absorption. *J Pharmacol Exp Ther.* 2001;297(2):638–45.
- Dixit RP, Nagarsenker MS. *In vitro* and *in vivo* advantage of celecoxib surface solid dispersion and dosage form development. *Indian J Pharm Sci.* 2007;69(3):370–7.
- Mamidi RNVS, Mullangi R, Kota J, Bhamidipati R, Khan AA, Katneni K, *et al.* Pharmacological and pharmacokinetics evaluation of celecoxib prodrugs in rats. *Biopharm Drug Dispos.* 2002;23(7):273–82.
- McAdam BF, Catella-Lawson F, Mardini IA, Kapoor S, Lawson JA, Fitzgerald GA. Systemic biosynthesis of prostacyclin by cyclooxygenase (COX)-2: the human pharmacology of a selective inhibitor of COX-2. *P Natl Acad Sci USA.* 1999;96(1):272–7.
- Humberstone AJ, Charman WN. Lipid-based vehicles for the oral delivery of poorly water soluble drugs. *Adv Drug Deliv Rev.* 1997;25(1):103–28.
- Pouton CW. Formulation of poorly water-soluble drugs for oral administration: physicochemical and physiological issues and the lipid formulation classification system. *Eur J Pharm Sci.* 2006;29(3–4):278–87.
- Hauss DJ. Oral lipid-based formulations. *Adv Drug Deliv Rev.* 2007;59(7):667–76.
- Ghouchi Eskandar N, Simovic S, Prestidge CA. Synergistic effect of silica nanoparticles and charged surfactants in the formation and stability of submicron oil-in-water emulsions. *Phys Chem Chem Phys.* 2007;9(48):6426–34.
- Ghouchi Eskandar N, Simovic S, Prestidge CA. Chemical stability and phase distribution of all-trans-retinol in nanoparticle-coated emulsions. *Int J Pharm.* 2009;376(1–2):186–94.
- Mohanraj VJ, Barnes TJ, Prestidge CA. Silica nanoparticle coated liposomes: a new type of hybrid nanocapsule for proteins. *Int J Pharm.* 2010;392(1–2):285–93.
- Tan A, Simovic S, Davey AK, Rades T, Prestidge CA. Silica-lipid hybrid (SLH) microcapsules: a novel oral delivery system for poorly soluble drugs. *J Control Release.* 2009;134(1):62–70.
- Simovic S, Heard P, Hui H, Song Y, Peddie F, Davey AK, *et al.* Dry hybrid lipid-silica microcapsules engineered from submicron lipid droplets and nanoparticles as a novel delivery system for poorly soluble drugs. *Mol Pharm.* 2009;6(3):861–72.
- Ghouchi Eskandar N, Simovic S, Prestidge CA. Nanoparticle coated submicron emulsions: sustained in-vitro release and improved dermal delivery of all-trans-retinol. *Pharm Res.* 2009;26(7):1764–75.
- Simovic S, Hui H, Song Y, Davey AK, Rades T, Prestidge CA. An oral delivery system for indomethacin engineered from cationic lipid emulsions and silica nanoparticles. *J Control Release.* 2010;143(3):367–73.
- Sanganwar GP, Gupta RB. Dissolution-rate enhancement of fenofibrate by adsorption onto silica using supercritical carbon dioxide. *Int J Pharm.* 2008;360(1–2):213–8.
- Mellaerts R, Mols R, Jammaer JAG, Aerts CA, Annaert P, Van Humbeeck J, *et al.* Increasing the oral bioavailability of the poorly water soluble drug itraconazole with ordered mesoporous silica. *Eur J Pharm Biopharm.* 2008;69(1):223–30.
- Wang F, Hui H, Barnes TJ, Barnett C, Prestidge CA. Oxidized mesoporous silicon microparticles for improved oral delivery of poorly soluble drugs. *Mol Pharm.* 2010;7(1):227–36.
- Prestidge CA, Barnes TJ, Lau C-H, Barnett C, Loni A, Canham L. Mesoporous silicon: a platform for the delivery of therapeutics. *Expert Opin Drug Deliv.* 2007;4(2):101–10.
- Brouwers J, Brewster ME, Augustijns P. Supersaturating drug delivery systems: the answer to solubility-limited oral bioavailability? *J Pharm. Sci.* 2009;98(8):2549–72.
- Guzman HR, Tawa M, Zhang Z, Ratanabanangkoon P, Shaw P, Gardner CR, *et al.* Combined use of crystalline salt forms and precipitation inhibitors to improve oral absorption of celecoxib from solid oral formulations. *J Pharm Sci.* 2007;96(10):2686–702.
- Adeyeye MC, Brittain HG. *Preformulation in solid dosage form development.* New York: Informa Healthcare; 2008.
- Sek L, Porter CJH, Charman WN. Characterisation and quantification of medium chain and long chain triglycerides and their *in vitro* digestion products, by HPTLC coupled with *in situ* densitometric analysis. *J Pharmaceut Biomed.* 2001;25(3–4):651–61.
- Schoenwald RD, editor. *Pharmacokinetics in drug discovery and development.* Boca Raton: CRC; 2002.
- Shchipunov YA. Lecithin organogel: a micellar system with unique properties. *Colloid Surface A.* 2001;183–185:541–54.
- Constantinides PP, Scalart J-P, Lancaster C, Marcello J, Marks G, Ellens H, *et al.* Formulation and intestinal absorption enhancement evaluation of water-in-oil microemulsions incorporating medium-chain glycerides. *Pharm Res.* 1994;11(10):1385–90.
- Puranajoti P, Patil RT, Sheth PD, Bommareddy G, Dondeti P, Egbaria K. Design and development of topical microemulsion for poorly water-soluble antifungal agents. *J Appl Res.* 2002;2(1):XXVII–XXVIII.
- Sari P, Razzak M, Tucker IG. Isotropic medium chain monodiglyceride/oil/water formulations for solubilization of lipophilic and hydrophilic drugs. *Int J Pharm.* 2004;270(1–2):287–96.
- Pieroni G, Verger R. Hydrolysis of mixed monomolecular films of triglyceride/lecithin by pancreatic lipase. *J Biol Chem.* 1979;254(20):10090–4.
- Seedher N, Bhatia S. Solubility enhancement of COX-2 inhibitors using various solvent systems. *AAPS PharmSciTech.* 2003;4(3):1–9.
- Dressman JB, Lennernas H. *Oral drug absorption: prediction and assessment.* New York: Marcel Dekker; 2000.
- Tan A, Simovic S, Davey AK, Rades T, Boyd BJ, Prestidge CA. Silica nanoparticles to control the lipase-mediated digestion of lipid-based oral delivery systems. *Mol Pharm.* 2010;7(2):522–32.
- Urum K, Pekdemir T. Evaluation of biosurfactants for crude oil contaminated soil washing. *Chemosphere.* 2004;57(9):1139–50.

36. Sek L, Porter CJH, Kaukonen AM, Charman WN. Evaluation of the in-vitro digestion profiles of long and medium chain glycerides and the phase behaviour of their lipolytic products. *J Pharm Pharmacol.* 2002;54(1):29–41.
37. Grubbs CJ, Lubet RA, Koki AT, Leahy KM, Masferrer JL, Steele VE, *et al.* Celecoxib inhibits N-butyl-N-(4-hydroxybutyl)-nitrosamine-induced urinary bladder cancers in male B6D2F1 mice and female Fischer-344 rats. *Cancer Res.* 2000;60(20):5599–602.
38. Friedman MI, Ramirez I, Tordoff MG. Gastric emptying of ingested fat emulsion in rats: implications for studies of fat-induced satiety. *Am J Physiol - Reg I.* 1996;270(3 39-3):R688–R92.
39. Porter CJH, Charman WN. *In vitro* assessment of oral lipid based formulations. *Adv Drug Deliv Rev.* 2001;50 Suppl 1:S127–S47.
40. Kaukonen AM, Boyd BJ, Porter CJH, Charman WN. Drug solubilization behavior during *in vitro* digestion of simple triglyceride lipid solution formulations. *Pharm Res.* 2004;21(2):245–53.